Received: 11 July 2019 | Revised: 5 September 2019 | Accepted: 24 September 2019

DOI: 10.1111/gcb.14875

PRIMARY RESEARCH ARTICLE

Global Change Biology WILEY

How afforestation affects the water cycle in drylands: A process-based comparative analysis

Kai Schwärzel[1,2] | Lulu Zhang[1] | Luca Montanarella[3] | Yanhui Wang[4] | Ge Sun[5]

[1]United Nations University Institute for Integrated Management of Material Fluxes and of Resources (UNU-FLORES), Dresden, Germany

[2]Thünen Institute of Forest Ecosystems, Eberswalde, Germany

[3]Joint Research Centre, European Commission, Ispra, Italy

[4]Research Institute of Forest Ecology, Environment and Protection, Chinese Academy of Forestry, Beijing, China

[5]Eastern Forest Environmental Threat Assessment Center, US Department of Agriculture Forest Service, Research Triangle, NC, USA

Correspondence
Kai Schwärzel, United Nations University Institute for Integrated Management of Material Fluxes and of Resources (UNU-FLORES), 01067 Dresden, Germany.
Emails: schwaerzel@unu.edu; kai.schwaerzel@thuenen.de

Funding information
Deutsche Forschungsgemeinschaft, Grant/Award Number: DFG Schw1448-3/1

Abstract

The world's largest afforestation programs implemented by China made a great contribution to the global "greening up." These programs have received worldwide attention due to its contribution toward achieving the United Nations Sustainable Development Goals. However, emerging studies have suggested that these campaigns, when not properly implemented, resulted in unintended ecological and water security concerns at the regional scale. While mounting evidence shows that afforestation causes substantial reduction in water yield at the watershed scale, process-based studies on how forest plantations alter the partitioning of rainwater and affect water balance components in natural vegetation are still lacking at the plot scale. This lack of science-based data prevents a comprehensive understanding of forest-related ecosystem services such as soil conservation and water supply under climate change. The present study represents the first "Paired Plot" study of the water balance of afforestation on the Loess Plateau. We investigate the effects of forest structure and environmental factors on the full water cycle in a typical multilayer plantation forest composed of black locust, one of the most popular tree species for plantations worldwide. We measure the ecohydrological components of a black locust versus natural grassland on adjacent sites. The startling finding of this study is that, contrary to the general belief, the understory—instead of the overstory—was the main water consumer in this plantation. Moreover, there is a strict physiological regulation of forest transpiration. In contrast to grassland, annual seepage under the forest was minor in years with an average rainfall. We conclude that global long-term greening efforts in drylands require careful ecohydrologic evaluation so that green and blue water trade-offs are properly addressed. This is especially important for reforestation-based watershed land management, that aims at carbon sequestration in mitigating climate change while maintaining regional water security, to be effective on a large scale.

KEYWORDS

afforestation, climate change, green and blue flows, soil and water conservation, soil erosion control, United Nations Sustainable Development Goals, water cycle in drylands, water scarcity management

1 | INTRODUCTION

Some regions of the earth are becoming greener as a result of climate warming, CO_2 fertilization, and land-use change (Chen et al., 2019; Zhang, Song, Band, Sun, & Li, 2017). One of these "greening up" regions is northwestern China, where the Chinese Government implemented the world's largest afforestation programs (Chen et al., 2018; Liu, Li, Ouyang, Tam, & Chen, 2008). These programs are planned until 2050 to reduce soil erosion and land degradation, adapt to climate change, alleviate poverty, and improve and restore land quality as well as watershed ecosystem services (Zhang & Schwärzel, 2017). One hotspot region for these programs is the Loess Plateau, which supplies a large amount of water and sediment for the lower reaches of the Yellow River. The Loess Plateau is the size of France and comprises up to 300 m thick loess deposits, which are wind-blown silt-sized sediments. Soils developed from loess are fertile and easily cultivated but extremely prone to erosion. Centuries of land use and severe soil erosion have led to more than 70% of the former flat plateau becoming a gully-hill dominated landscape (Zhao, Mu, Wen, Wang, & Gao, 2013). Bryan et al. (2018) reviewed China's investment strategies for land-system sustainability and concluded that the large-scale afforestation programs were successful and set a world example to address future challenges; however, the afforestation had led to unintended local and regional water shortages. This is alarming for the health of Asia's third largest river, the Yellow River.

Analyses on streamflow and land-use change as well as numerous modeling studies at the catchment scale (Feng et al., 2012; Sun et al., 2006; Zhang et al., 2014) show that land-use change plays a bigger role for observed water yield reductions than does climate change. Although a growing number of plot-scale studies quantify soil water storage alterations due to afforestation (Jia, Shao, Zhu, & Luo, 2017; Liu et al., 2018; Yang, Wei, Chen, & Mo, 2012), none address the interplay of rainfall, evapotranspiration, soil water dynamics, and seepage of dryland forest plantations. There are no rigorous process-based comparative measurement studies on how forest plantations affect the water balance components and alter partitioning of rainwater into green (evapotranspiration) and blue water flows (surface and subsurface). Wang et al. (2012) pointed out that the relationship between woody plants, understory, and soil water is barely understood, and the degree to which one offsets another relies on the scale at which these impacts are quantified. Newman et al. (2006) also argued that our understanding of feedback and interactions between biotic and hydrologic components of environmental systems depends mainly on ecosystem process models, and a lack of data has restricted their application. For instance, little is known about the partitioning of evaporative fluxes in dryland afforestation (Gimeno, McVicar, O'Grady, Tissue, & Ellsworth, 2018) when this would provide a deeper understanding of the biological regulation of the hydrological cycle and the impact of soil water dynamics on vegetation performance (Huxman et al., 2005; Kool et al., 2014; Newman et al., 2006).

Black locust (*Robinia pseudoacacia* L.) is a major tree species for plantations on the Loess Plateau. Its good growth attributes have made it one of the most commonly cultivated deciduous tree species worldwide. It is native to North America and has been introduced to many different regions for wood, fuel, forage, and beekeeping. Black locust rivals poplar as the second most planted broadleaved tree species worldwide, after the eucalypts (Redei et al., 2018). Black locust was introduced in China early in the 20th century and is now widely used for afforestation as a pioneering tree species (Wang, 1992). Currently, it represents >90% of plantation forests on China's Loess Plateau (Ma et al., 2017). However, water balance studies on black locust plantations are rare, and moreover, published water consumption data for this species are often biased. In earlier works (Podlasly & Schwärzel, 2013; Schwärzel, Zhang, Strecker, & Podlasly, 2018), we developed a specific calibration method to improve the estimation of the water consumption of black locust and implemented field experiments that partitioned evapotranspiration of black locust stands with understory.

Consequently, here we focus on (a) how the overstory and understory contribute to the total water consumption of black locust plantations, (b) which environmental factors control the various evaporative fluxes, and (c) if and to what extent black locust plantations alter the water cycle. To address these points, we use established ecohydrological measurements of black locust plantations versus natural grassland (as a reference system) at adjacent sites under the same soil, topography, and climate conditions (Yu et al., 2015). Our work will contribute to addressing data gaps on feedback and interactions between biotic and hydrologic components in water-limited environments.

2 | MATERIALS AND METHODS

2.1 | Study site

The small 14 km^2 watershed of Zhonggou is in the gully area of the Loess Plateau at 1,000–1,300 m above sea level and discharges into the Jinghe basin, Gansu Province. Soils in this catchment developed from loess deposits of thickness 50–80 m. The soil is classified as Calcaric Regosol (IUSS Working Group WRB, 2006) with silt loam texture (Yu et al., 2015). The climate of the region is semi-humid. Records of Jingchuan Hydrological Station (1990–2007) show the following annual mean values: temperature of 10.2°C, potential evapotranspiration of 1,395 mm, and precipitation of 590 mm. The vegetation period begins at the end of April and ends in mid-October. Of the catchment area, 83% is covered by forest, mainly black locust. At our site, black locust was planted in the 1970s, but has regenerated through resprouting after a clear cut in 1990. The study plot covered 2,700 m^2 and included 206 trees with a basal area of 8.2 m^2/ha. The summer maximum leaf area index (LAI) of the stand ranged within 2.7–2.9 (measured using LAI 2000-PCA, LI-COR Inc.). In 2012, the average tree height and diameter at breast height (DBH) were 11.8 m and 10.7 cm, respectively. The understory consists mainly of grass (*Melilotus suaveolens*, *Astragalus adsurgens*, *Onobrychis taneitica*, *Equisetum arvense*,

Juncus bufonius, *Pennisetum centrasiaticum*, *Phragmites communis*, *Setaria viridis*, and *Chenopodium album*), but some shrubs such as *Amorpha fruticosa*, *Prunus davidiana*, *Hippophae rhamnoides*, *Syringa persica*, *Caragana korshinskii*, and *Xanthocera sorbifolia* can also be found. Adjacent to the forest, there is a grassland with dominant species of *Artemisia argyi H. Lév. & Vaniot*, *Pennisetum centrasiaticum Tzvelev*, *Arundinella anomala Steud.*, *Achnatherum sibiricum* (L.) *Keng ex Tzvelev*, *Jasminum nudiflorum Lindl.*, *Medicago minima* (L.) *Grufberg*, and *Tripolium vulgare Nees*. Summer maximum LAI of the understory ranged within 3.2–3.6 (measured as described above).

2.2 | Weather stations

An open-land weather station was installed in 2012, ~300 m east of the black locust plantation. Global and net radiation (Kipp & Zonen), air temperature, relative humidity, wind direction and speed (Thies), and soil temperature at the soil surface and different depths were recorded in 15 min intervals. Rainfall was measured using a tipping bucket system with heating (Lambrecht). Air and soil temperature, relative humidity, and global and net radiation were also measured under the black locust canopy. Two stainless steel throughfall troughs (5 m long, 0.16 m wide) draining into a tipping bucket were installed beneath the canopy and operated from the end of March until mid-October.

2.3 | Soil water conditions

To measure soil water dynamics, a wireless sensor network (FZ Jülich) was installed under the black locust canopy and on the grassland. Soil moisture was measured using a spade sensor (sceme.de GmbH) with a measurement resolution of 0.01 (L^3/L^3; Qu, Bogena, Huisman, & Vereecken, 2013). (For details of sensors and their installation, see Schwärzel et al., 2018.) At each site, 36 spade sensors were installed at six depths at a horizontal distance of 60 cm apart. Sensors were placed at depths of 5, 20, and 40 cm (eight replications), and 60, 80, and 100 cm (four replications). Soil moisture sensors operated from the end of March until the end of September. For technical reasons, there were no soil moisture data from mid-April to the end of May 2012. Soil pressure head was measured under the canopy and grassland at depths of 20, 40, 60, and 80 cm using *pF*-meter (ecoTech), which measures heat capacity in a porous equilibrium body, from which soil pressure head values are derived.

2.4 | Understory and grassland evapotranspiration

To quantify water consumption of understory and grass, two weighable field lysimeters were installed: one under the black locust canopy and one on the grassland. The lysimeter comprised a polyethylene container (2.50 × 2.30 × 1.50 m); a stainless steel lysimeter vessel (surface area 1.0 m^2, length 1.70 m) filled with undisturbed soil; a weighing system; and a unit to automatically regulate soil moisture and temperature at the lower bottom of the lysimeter. (For details of lysimeter installation and automated control of its lower boundary, see Podlasly and Schwärzel, 2013.) Decreases in lysimeter weight (logged every 30 min) were caused by root water uptake and soil evaporation. Thus, we use understory evapotranspiration (ET_{us}) and grassland evapotranspiration (ET_{grass}) when referring to water consumption quantified by the lysimeter, calculated as follows:

$$ET_{us} = P_{net} - D - \Delta M/\rho_w \pi r^2 + \Delta T, \quad (1)$$

$$ET_{grass} = P - D - \Delta M/\rho_w \pi r^2 + \Delta T, \quad (2)$$

where P_{net} is net precipitation (measured by throughfall troughs), P is open-land precipitation (L/T), D is drainage water collected at the lysimeter bottom (L/T), ΔM is change of lysimeter mass (1 M/T = 1 L^3/T), ρ_w is water density (M/L^3), r is lysimeter radius (L), and ΔT is the amount of water added to control pressure head at the lower bottom of the lysimeter (L/T).

2.5 | Overstory transpiration

Granier-style sap flow sensors were used to quantify stand contribution to total evapotranspiration. Probes were 20 mm long with diameter 1.5 mm (Ecomatik). Fourteen trees were equipped with sap flow sensors. (For installation details, see Schwärzel et al., 2018.) Temperature differences between the heated and unheated needles were measured in 60 s intervals and data logged as 60 min averages. Hourly sap flow densities, F_d ($L^3/L^2 \cdot T$), were calculated from observed temperature differences using Equation (3) (Granier, 1985):

$$F_d = a \times \left(\frac{\Delta T_M - \Delta T}{\Delta T} \right)^b, \quad (3)$$

where ΔT (K) is measured temperature difference between the two needles, ΔT_M (K) is ΔT value at F_d = 0, and coefficient a and exponent b are fitting parameters. Instead of Granier's original parameters, tree-specific parameters derived from in situ calibration on a living tree at our experimental plot (Schwärzel et al., 2018) were used to convert observed temperature differences into sap flow densities. Additionally, we used the soil water balance method to test the reliability of the tree-specific calibration. The coefficient a obtained from the fit was 3.29 kg $m^{-2}s^{-1}$, and the parameter b was very similar to the 1.231 reported by Granier (1985). To consider potential nocturnal fluxes due to both transpiration and recharge, ΔT_M was estimated according to Lu, Urban, and Zhao (2004) and determined using BaseLiner software (Schwärzel et al., 2018). No functional relationship between the daily total sap flow density and corresponding DBH was found. Thus, daily sap flow densities of all sample trees were averaged to estimate daily transpiration (T_{BL}) of the black locust stand (mm/day) using averaged flux densities (J_{avg}), total sapwood area of the plot (A_{ST}), and stand ground surface (A_G; Clausnitzer, Köstner, Schwärzel, & Bernhofer, 2011):

$$T_{BL} = J_{avg} \times \frac{A_{ST}}{A_G}. \quad (4)$$

To determine conducting sapwood, 10 trees—with DBH similar to trees used for sap flow measurement—were harvested and

corresponding tree-ring widths of the outermost rings were measured using stem disk at breast height. Regression between DBH and corresponding sapwood area was used to calculate total sapwood area of the plot using the frequency of tree DBH. The tree-cutting technique was applied to visualize water-conduction pathways in living black locust trees (Schwärzel et al., 2018).

2.6 | Seepage

We applied three different methods to estimate seepage: (a) lysimeter method, (b) zero-flux-plane (ZFP) method, and (c) calculation of annual seepage rate as residual of the field water balance in the surface soil zone of the grassland and forestland site at a level position (i.e., no surface runoff). The latter can be described as:

$$S_{\text{grass}} = P_{\text{gross}} - \text{ET}_{\text{grass}} - \Delta W, \quad (5)$$

$$S_{\text{forest}} = P_{\text{gross}} - P_{tf} - I - \text{ET}_{\text{us}} - T_{\text{black locust}} - \Delta W, \quad (6)$$

where S is seepage/deep percolation below the soil zone, P_{gross} is precipitation on open land, P_{tf} is throughfall, I is canopy interception of rainfall, and ΔW is water storage change in the soil profile.

Terms in Equations (5) and (6) represent water fluxes or storage changes over any time interval. Annual soil water storage changes are usually minor in humid and semi-humid environments. The annual amount of seepage under grass and forest can thus be calculated as residual using the measured fluxes as described above. The sum of annual drainage water, D, collected at the bottom of the lysimeters under grass corresponds to annual seepage. For shorter time intervals, soil water storage changes must be considered when estimating seepage under forest and grassland; additionally, evapotranspiration and drainage can occur simultaneously. Consequently, the ZFP method was applied using the soil water content and soil pressure head measurements as a function of time and depth as described above. ZFP is defined as a plane separating two zones of upward and downward movement of water in unsaturated soils with simultaneous evapotranspiration and seepage (Khalil, Sakai, Mizoguchi, & Miyazaki, 2003). If ZFP is located below the root zone, soil moisture changes above the ZFP are due to evaporation from soil and root water uptake, whereas soil moisture changes below the ZFP are caused by seepage. A limitation of the ZFP method is preferential flow during storm events, implying that much of the soil above the ZFP is bypassed whereas soil below the ZFP is wetted (Cooper, Gardner, & Mackenzie, 1990; Schwärzel et al., 2009). Under such circumstances, this method would overestimate evapotranspiration and underestimate seepage (Cooper et al., 1990). At our site, preferential flow was important in the recharge of plant-available soil water and seepage, as indicated by a rapid decline in soil pressure head at depth of 80 cm in September 2012, July 2013, and September 2013 (Figure 1). Consequently, ΔW in Equations (5) and (6) was not determined on a daily timescale but calculated—as the difference in soil water storage at the beginning and end of the balance period—over the entire period in which a ZFP existed and the hydraulic gradient below the main root zone indicated

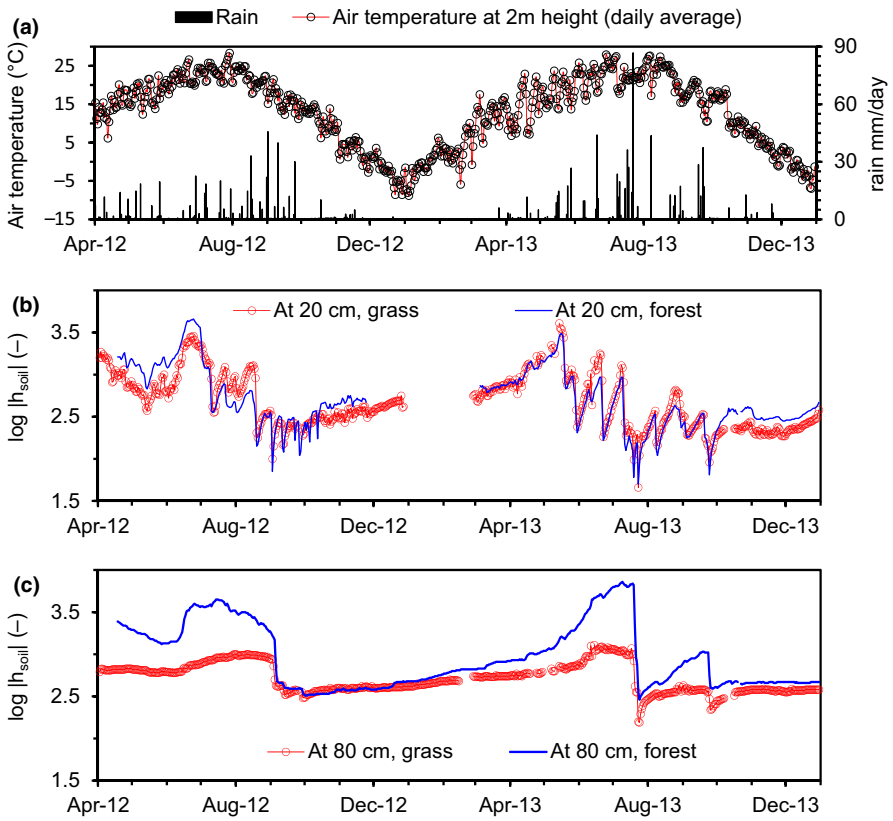

FIGURE 1 (a) Daily air temperature at height of 2 m, open-land rainfall and (b, c) soil moisture conditions (*pF* value = logarithm of soil pressure head) under forest and grassland at soil depth of 20 (1b) and 80 cm (1c)

downward movement of water. The daily values of rainfall and evaporation components of Equations (5) and (6) were summed for these balance periods.

2.7 | Data gap filling and further calculations

Due to occasional instrument failure and unfavorable weather, data gap-filling was needed. Meteorological data were obtained from the Changwu Agro-Ecological Experimental Station (30 km from our field) and regression analyses applied to calculate missing data. In a very few cases, the canopy or grassland lysimeter delivered no or implausible data and these gaps were filled by regressions using data from the other lysimeter. Missing overstory transpiration data were filled by hydrological modeling using BROOK90 (Federer, Vörösmarty, & Fekete, 2003), which estimates daily interception, transpiration, evaporation, seepage, snow accumulation, and snow melt. Partitioning of evapotranspiration is based on the Shuttleworth–Wallace equation. Reliability of estimations and detailed gap filling procedures are presented in supplementary materials. To determine the extent that vegetation controls evaporation, decoupling factors were calculated following Jarvis and McNaughton (1986; detail in supplementary materials). The decoupling coefficient ranges within 0–1. Values close to 0 indicate strong vegetation–atmosphere coupling, with vapor pressure deficit, VPD as the main driver of evaporation. For values close to 1, vegetation is decoupled from the atmosphere; then, net radiation is the main driver for evaporation.

3 | RESULTS

3.1 | Weather and soil water dynamics during the study

Atmospheric evaporative demand during the main growing season (May–September)—characterized by grass reference evapotranspiration—was significantly lower (770 mm) in 2012 and slightly lower (810 mm) in 2013 than the long-term average (840 mm). This was partly due to higher seasonal rainfall (460 mm in 2012 and 630 mm in 2013) than the long-term average (420 mm). Figure 1a shows a distinct temporal pattern of rainfall.

There was almost no rainfall between the end of September and the beginning of April. In contrast, 60%–80% of annual rainfall occurred during June–September mostly in heavy falls (Figure 1a). For instance, from the end of May to the end of September 2012, there were 13 storm events of >10 mm rainfall which accounted for 78% (290 mm) of the total rainfall during this rainy season. The only noteworthy difference in temperature regimes between years (Figure 1) was that daily air temperature varied more in 2013, particularly during the rainy season. The *pF*-values increased in periods with no or little rainfall and high evaporation demand of the atmosphere and decreased during and after rainfall events (Figure 1b,c). The *pF*-data revealed several noteworthy points. First, temporal courses of *pF* at depth of 20 cm under grassland and forest were quite similar, and topsoil soil pressure heads responded immediately to storm events (Figure 1b). Second, due to high seasonal rainfall in 2013, topsoil under both vegetation covers was wetter than in 2012, except during April–May (Figure 1b). Third, there were important differences in soil water dynamics (in terms of soil pressure head) between vegetation covers in subsoil compared to topsoil (Figure 1c). In both years, soil pressure head at depths of 60 (not shown) and 80 cm under forest increased significantly as soon as the black locust canopy fully developed (second half of May). Compared to forest, there was just a slight increase of soil pressure head at the depth of 80 cm under grassland (Figure 1c). Fourth, the decrease in soil pressure heads at all depths at the end of seasons indicates that depleted soil water was gradually recharged by rain until the end of September (Figure 1b,c). Finally, in late fall 2012 and 2013 and early winter 2012, soil was at field capacity, with similar soil pressure head at all depths (*pF* 2.5–2.7).

The temporal course of the ratio between net radiation at the forest floor and the grassland is largely controlled by the presence of leaves of the forest canopy (Figure 2a). During the dormant season (end of October to mid-April), net radiation at the forest floor was about 70% of the value at the grassland site (Figure 2a). Immediately before budburst (second half of April), net radiation at the forest floor increased with sun angle to about 90% followed by a fast decrease in May with crown development. During June–August, with the canopy fully developed, net radiation at the forest floor was ~29% (2012) and ~25% (2013) of grassland values. Due to leaf fall in late summer and fall, the ratio of net radiation at the forest floor to that at the grassland gradually increased to 70% by the end of December. Canopy cover development also affected air temperature and VPD below the canopy (Figure 2b,c). Because of canopy shading and evaporation from the forest floor, daily air temperatures and VPDs below the canopy were lower during the growing season compared to grassland (Figure 2b,c); however, VPD at the forest floor remained high as shown by small differences in VPD between forest floor and grassland (Figure 2c). This indicates a significant degree of coupling through the forest canopy layer.

3.2 | Diurnal and seasonal variations of evaporative fluxes

There was a stark contrast in evaporation among overstory, understory, and grass as shown for the two hot sunny days without rainfall before (16 June) and after (14 July) the onset of the rainy season in 2012 (Figure 3). On these days, the canopy was fully developed and meteorological conditions—diurnal courses of global radiation, air temperature, and VPD and daily averages of weather variables—were comparable (Figure 3a,b and Table 2). However, soil water conditions for these 2 days differed significantly (Figure 3c,d). Because of a long period with little rainfall (28.8 mm between 11 May and 16 June) and high evaporation demand of the atmosphere, topsoil under grass, and forest dried as shown by increased *pF* (Figure 3c,d). The *pF*-values

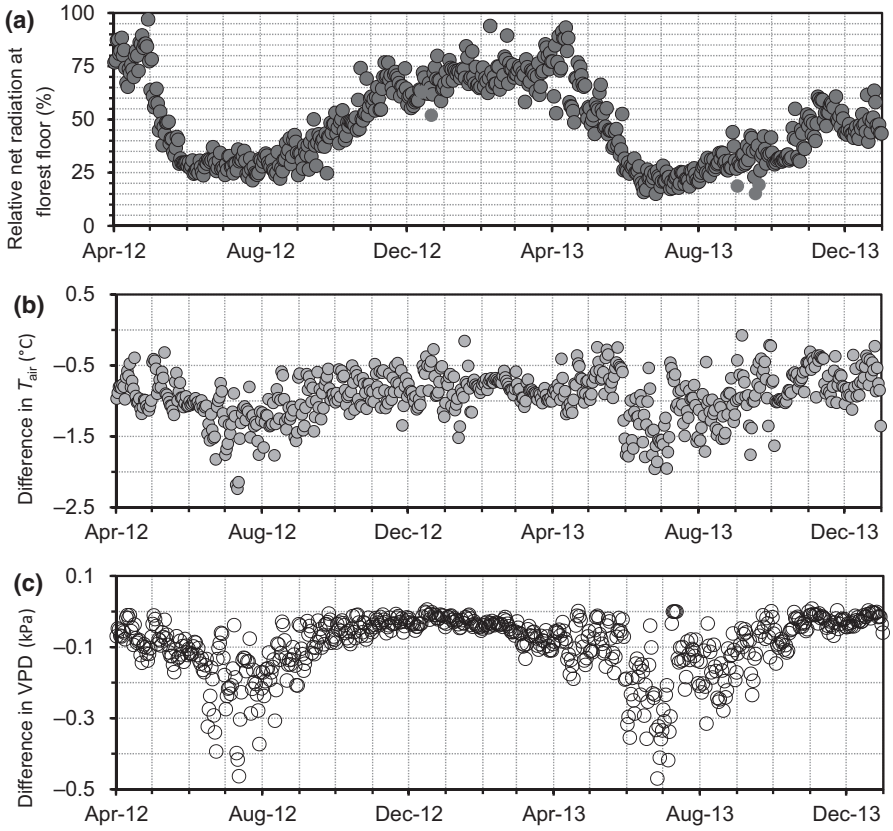

FIGURE 2 (a) Daily values of the ratio of net radiation at the forest floor to that at the grassland site and (b) absolute differences in daily air temperature and (c) VPD between forest floor and grassland

dropped from about 3.5 (16 June) to 2.7 on 14 July because of 125 mm of rainfall between the end of June and mid-July. Overstory transpiration increased from early to late morning, leveled off before noon, and was then unvarying by late afternoon (Figure 3e,f).

Thus, despite significant changing atmospheric boundary conditions during the day, transpiration rates remained stable when the daily maximum rate was approached (Figure 3e,f). This contrasts markedly with grassland and forest floor evaporation rates, which increased sharply with increasing VPD and peaked in the afternoon around the same time as VPD reached its daily maximum (Figure 3e,f). Moreover, grass and forest floor had substantially higher evaporation rates than overstory. Notably, the early morning peaks in evaporation from grass and understory were from evaporation of dew formed overnight. Evaporation rates were used to calculate surface conductance of the different vegetation covers. The surface conductance of the overstory generally peaked in the morning, declined before noon, and remained low in the late afternoon (Figure 3g,h).

Overstory conductance showed little sensitivity to changes in soil moisture (Figure 3g,h). Contrary to the latter, evaporation from grassland responded to increased soil water availability (characterized by *pF*-values): under dry soil conditions (16 June), the ratio between daily evaporation from grassland to daily grass reference evapotranspiration was 67% (Table 1), but for wetter soil (14 July), the ratio was 87%. For understory and overstory evaporation, the ratios between measured evaporation and calculated grass reference evapotranspiration remained unchanged under changing soil water conditions (Table 1). Compared to overstory and grassland, understory conductance often had a multipeaked daily cycle with maxima before noon and late afternoon (Figure 3g,h). Furthermore, conductance varied much more throughout the day for understory and overstory than grassland. The coefficient of variation of canopy conductance was 50% for overstory and understory, and <20% for grassland.

Figure 4a,b shows an example of seasonal variation in daily fluxes of evaporation of the contrasting vegetation covers during April–October 2012. Due to canopy shading, daily evaporation rates were usually lower for understory than grassland; however, the differences were small (Figure 4a,b). Furthermore, daily values of overstory transpiration (Figure 4b) were markedly lower than grassland (Figure 4a) and understory evaporation (Figure 4b).

The highest fluxes were during June–August with daily maxima of 4.7 mm for grassland evaporation, 3.7 mm for understory evaporation, and 1.8 mm for overstory transpiration. During June–August, daily mean evaporation from grassland, understory, and overstory was 2.5, 1.8, and 1.1 mm, respectively. Low daily evaporation rates were generally associated with rainfall. Daily rates of overstory transpiration varied considerably less than evaporation from grassland or understory (Figure 4b). During June–August, the coefficient of variation of daily overstory transpiration was 30%, compared to 48% for grassland and 50% for understory. These differences among vegetation covers could be caused by different mechanisms of evaporation control, as discussed in the next section.

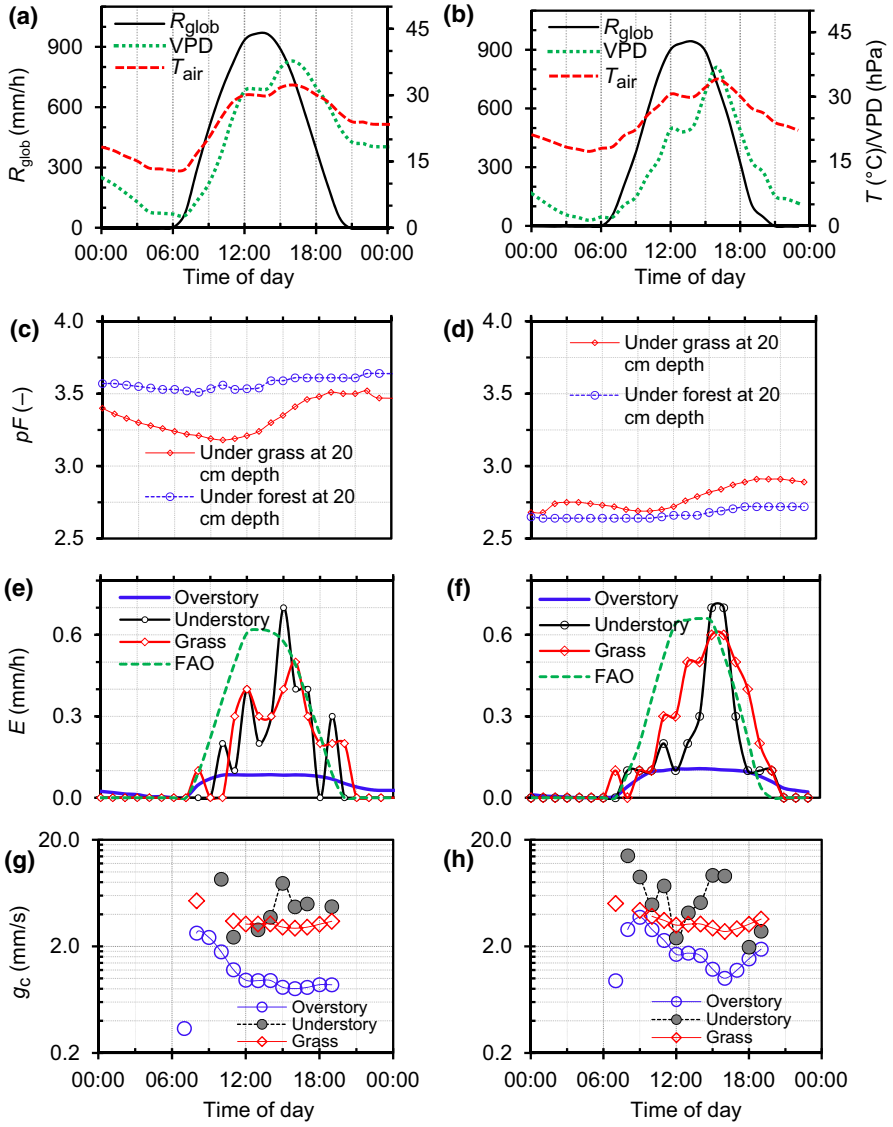

FIGURE 3 (a, b) Hourly weather data for the open-land weather station (global radiation, Rglob; air temperature, Tair; vapor pressure deficit, VPD), (c, d) hourly logarithm of soil pressure head (*pF*) at the depth of 20 cm under grass and forest, (e, f) hourly evaporation data (tree transpiration, understory, grassland evapotranspiration, and FAO grass reference evapotranspiration), and (g, h) hourly data of canopy conductance (g_c) of the black locust stand, understory, and grassland for sunny days before (16 June, left side) and during (14 July, right side) the rainy season in 2012. No rainfall on the selected days

TABLE 1 Meteorological data, measured daily evaporative fluxes, and derived mean canopy conductance for sunny days without rainfall before (16 June) and during (14 July) the rainy season 2012

	R_N (W/m^2)		T_{air} (°C)		VPD (KPa/K)		*E* (mm/day)				g_c (mm/s)		
Date	Above canopy	Below canopy	Above canopy	Below canopy	Above canopy	Below canopy	Overstory	Understory	Grass	FAO	Overstory	Understory	Grass
June 16, 2012	349	129	27.9	25.8	2.67	2.17	1.2	3.0	3.2	4.7	1.2	5.2	5.0
July 14, 2012	380	129	28.7	26.2	2.01	1.53	1.3	3.1	4.3	4.9	1.9	5.9	6.4

Note: Hourly data are presented in Figure 3.

3.3 | Influence of environmental conditions on evaporation

The relationship between daytime data of net radiation and daily evaporation rates of the contrasting vegetation covers was plotted for June–August 2012 and 2013 when the canopy was fully developed (Figure 5). Clearly, overstory transpiration was a maximum at net radiation of 15 MJ m^{-2} day^{-1} (Figure 5a), whereas evaporation from grassland (Figure 5b) and understory (Figure 5c) was largely controlled by radiation. However, compared to grassland, understory data were much more scattered. In general, differences in relationships between radiation and evaporation for the contrasting vegetation covers can be attributed to differences in stomatal control of evaporation. For a better understanding of the latter, surface

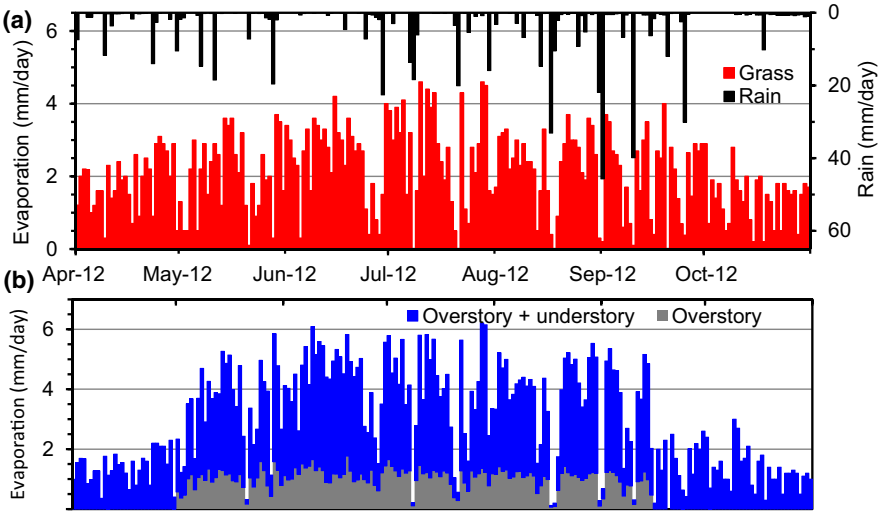

FIGURE 4 (a) Daily values of grassland evaporation and open-land rainfall (above), (b) daily sums of overstory and understory evaporation, and overstory evaporation alone (below) for 2012 growing season

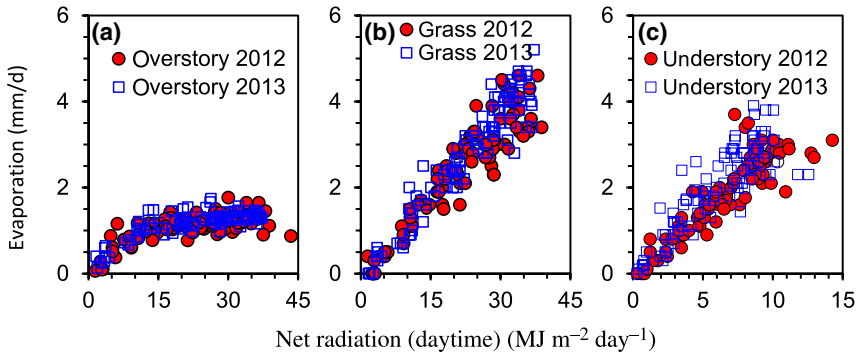

FIGURE 5 Relationship between daily evaporation and daytime net radiation for (a) overstory, (b) grass, and (c) understory for days without rainfall during 2012 and 2013 growing seasons

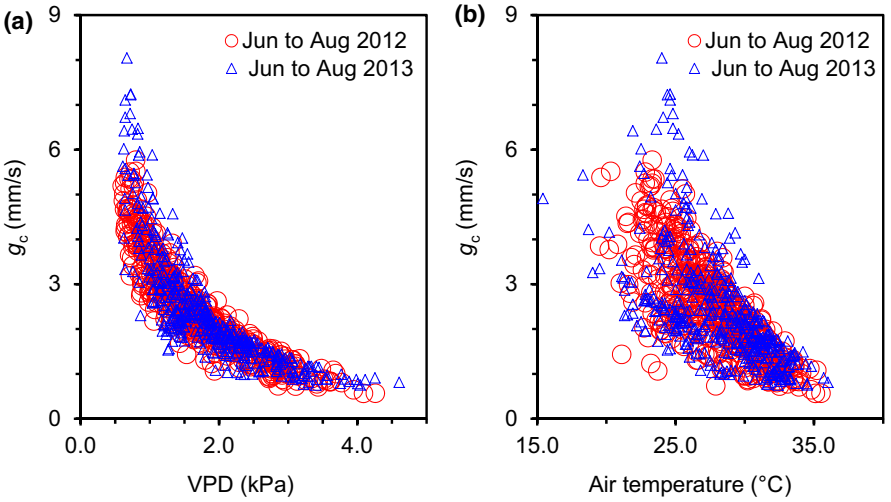

FIGURE 6 Relationship (a) between black locust surface conductance (g_c) and VPD (left), and (b) between g_c and air temperature (right). Shown are hourly data for periods without rainfall

conductance of grassland, understory, and overstory was estimated on an hourly basis as previously outlined.

Figure 6 shows the dependency of overstory conductance on VPD (Figure 6a) and air temperature (Figure 6b) for June–August 2012 and 2013. Overstory transpiration was largely controlled by VPD (R^2 = .84 in 2012 (not shown) and .88 in 2013) and to a lesser extent by air temperature—for air temperatures >30°C, R^2 = .45 in 2013 (not shown) and .60 in 2012. As discussed earlier, understory surface conductance often had a multipeaked daily cycle (Figure 3). Moreover, for understory and grassland, there was a diurnal hysteresis between maximum net radiation and maximum evaporation, and between maximum VPD and maximum evaporation, which differed

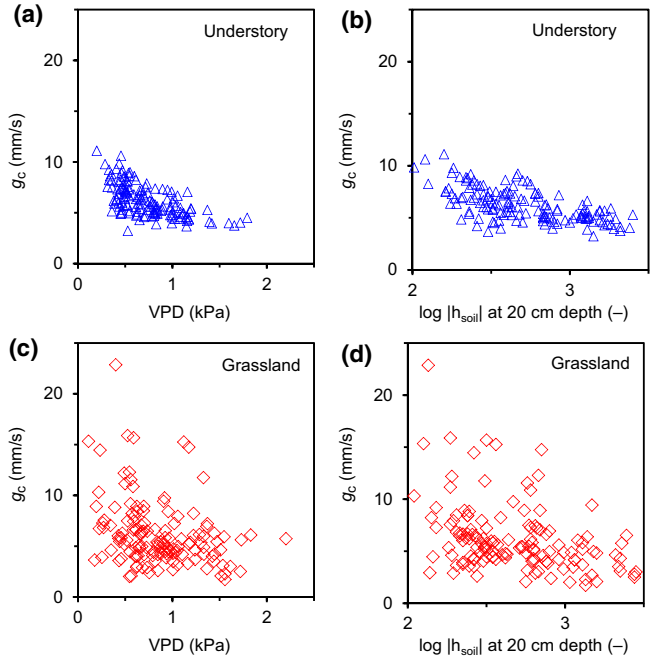

FIGURE 7 Relationship (a, c) between daily means of canopy conductance (g_c) and vapor pressure deficit, VPD, and (b, d) between daily means of g_c and the logarithm of soil pressure head (log |hsoil|) at depth of 20 cm for understory (a, b) and grassland (c, d). Shown are daily data for days with rainfall < 1 mm during 2012 and 2013 growing seasons

throughout the season. Consequently, no relationships between understory/grassland conductance and meteorological variables were found using hourly data. Thus, daily averages of understory and grassland conductance were plotted against daily averages of environmental variables.

There was a moderate relationship of understory conductance with VPD (R^2 = .50, not shown) and with soil pressure head (R^2 = .48, not shown; Figure 7a,b). This indicated that daily understory evaporation was not just controlled by radiation as discussed above (Figure 4) but also by VPD and soil moisture conditions. In contrast to understory, only a weak relationship between VPD and grassland conductance (R^2 = .10, not shown) was observed (Figure 7c), but Figure 7d revealed a trend for grassland conductance to decrease markedly when topsoil under grassland dried up (pF > 3.0, R^2 = .19, not shown). It was discussed above that grassland transpiration was largely controlled by radiation (Figure 4). However, Figure 7d indicates that soil water conditions had strong control over the evaporation flux from grassland if a certain soil water deficit was reached (characterized by the soil pressure head of topsoil). This was discussed above concerning the diurnal dynamics of evaporative fluxes (Figure 3).

3.4 | Field water balance of contrasting vegetation covers

The water balance components for each month are shown in Table 2.

The lack or presence of leaves of the forest canopy controls the partitioning of evaporation as well as of rainfall. During the leafless period from the end of October to mid-April, differences in evaporation between the contrasting vegetation covers were relatively small. Large discrepancies in evaporation between the contrasting vegetation covers were observed as soon as the canopy was fully developed in May. This was due to the combination of overstory transpiration, evaporation of rainwater intercepted by the forest canopy, and evaporation from the understory.

The ET_{us} was 264 mm in 2012 and 273 mm in 2013 (May–September). Despite canopy shading, differences between ET_{us} and ET_{grass} were quite small: 24% in 2012 and 28% in 2013. The ET_{us} accounted for >50% of total seasonal forest evapotranspiration ETI (53% in 2012 and 56% in 2013). The ET_{grass} represented 60% (2013) and 75% (2012) of seasonal rainfall whereas forestland (without interception) was correspondingly 69% and 90%. Interception of rainfall by the canopy was low because most rainfall during the season was heavy showers (Figure 1). Moreover, despite important differences in evaporation demand of the atmosphere and rainfall in 2012 and 2013, there were only small variations in total seasonal evapotranspiration of the contrasting vegetation cover.

Figure 8 shows temporal changes in the hydraulic gradient below the main root zone for the contrasting vegetation covers. A negative hydraulic gradient indicates that soil water moved upwards toward the root zone whereas a positive gradient indicates downward movement. Water draining through any depth below the root zone will eventually contribute to groundwater recharge. At the grassland site, water moved from the subsoil to the root zone and soil surface in spring and early summer (Figure 8). During this time, root water uptake by grass exceeded the rainfall amount. With the onset of the rainy season, an abrupt reversal in direction of water movement below the root zone of the grassland occurred in mid-July 2012 and at the beginning of June 2013—revealing that seepage had taken place. For the grassland, we estimated seepage of 30 mm in 2012 and 188 mm in 2013 using the ZFP method. In contrast to soil under grass, no seepage occurred under forest in 2012 although for a short period, there was downward movement of water (Figure 8). It was previously mentioned that the rainy season in 2013 was unusually wetter than average. For this reason, seepage of 63 mm under forest was found in 2013; however, this only occurred from the end of June to the end of July, when rainfall exceeded evapotranspiration (Figure 9). Compared to the ZFP method, the lysimeters collected significant drainage water with a time lag between 4 (under forest) and 8 (under grass) weeks (Table 2). This lag is because drainage water collected at a depth of 1.75 whereas the ZFP method balances soil water storage changes over a depth of 1 m.

Partitioning of annual rainfall in grassland and forestland showed that black locust plantation lost 92% of annual rainfall as ETI, and grassland lost 80% (Figure 9). Under the forest, most water was taken up by the understory, representing 58% of annual rainfall compared to only 26% by tree roots. Canopy interception was low (8%) due to frequent rainstorm events. Annual seepage—calculated as residual

TABLE 2 Measured monthly water balance components

				T_{BL} + ET_{us} + I					Drainage lysimeter	
Year	Month	P_{gross} (mm)	P_{net} (mm)	ET_{grass} (mm)	ETI_{forest} (mm)	I (mm)	ET_{us} (mm)	T_{BL} (mm)	Grass (mm)	Forest (mm)
2012	April	58.3	56.6	55.2	50.9	1.7	42.2	7.0	0.0	0.0
	May	70.3	61.3	63.0	86.0	9.0	47.1	29.9	0.0	0.0
	June	40.6	34.2	75.0	102.7	6.4	61.2	35.1	0.0	NM
	July	88.3	78.5	81.4	98.6	9.8	55.4	33.4	0.0	NM
	August	113.8	92.1	71.2	106.4	21.7	53.6	31.1	0.0	NM
	September	150.7	120.4	59.4	102.2	30.3	47.0	24.9	23.2	NM
	October	21.9	12.6	43.2	62.1	9.3	40.1	12.7	23.4	NM
	November	3.2	0.0	8.0	13.9	8.1	5.8	0.0	0.0	0.9
	December	1.3	0.0	0.9	1.9	0.5	1.4	0.0	0.0	0.0
	May–September	**463.7**	**386.5**	**350.0**	**495.9**	**77.2**	**264.3**	**154.4**	**23.2**	–
	April–December	**548.0**	**456.0**	**457.3**	**618.6**	**90.7**	**353.8**	**174.1**	**46.6**	–
2013	January	0.0	0.0	2.1	3.5	0.0	3.5	0.0	0.0	0.0
	February	0.0	0.0	3.7	4.2	0.0	1.5	0.0	0.0	0.0
	March	6.5	6.4	25.4	20.0	0.1	19.9	0.0	0.0	0.0
	April	31.6	27.5	71.4	62.1	4.1	52.8	5.2	0.0	1.4
	May	89.1	79.1	75.0	97.9	10.0	56.0	31.9	0.0	0.8
	June	84.2	78.7	87.9	103.5	5.5	61.9	36.1	0.0	0.7
	July	250.1	234.2	68.7	97.4	15.9	47.3	34.2	40.2	14.5
	August	76.1	76.5	100.3	107.8	0.0	70.4	37.4	65.0	15.7
	September	127.4	110.2	46.4	77.6	17.2	37.3	23.1	17.6	26.0
	October	24.5	21.7	52.1	56.2	2.8	37.8	15.6	23.6	1.2
	November	17.8	17.6	18.6	13.1	0.2	12.9	0.0	16.7	5.6
	December	0.0	0.0	8.4	4.2	0.0	4.2	0.0	5.6	3.0
	May to September	**627.0**	**578.7**	**378.3**	**483.8**	**48.3**	**272.9**	**162.6**	**127,2**	**57.7**
	April to December	**697.3**	**642.2**	**528.8**	**621.5**	**57.4**	**380.6**	**183.5**	**178.0**	**68.9**

Bold value indicates the differences between 2012 (normal year) and 2013 (wet year).

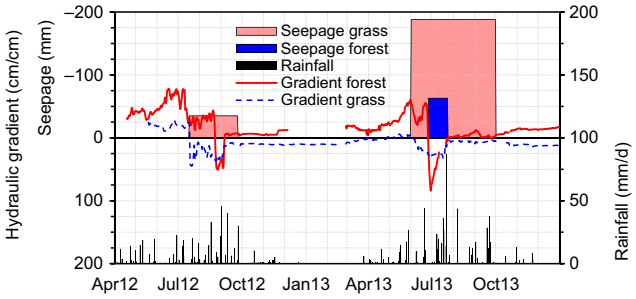

FIGURE 8 Seasonal changes in hydraulic gradient below the main root zone at depth of 70 cm under forest and grass, daily rainfall, and the sum of seasonal seepage (negative numbers) under grass and forest estimated using Equations (5) and (6). Positive hydraulic gradient indicates downward flow of water, and a negative gradient indicates upward flow

of the field water balance (Equations 5 and 6)—differed significantly under forest (8% or 56 mm) and grassland (20% or 140 mm) in this wet year.

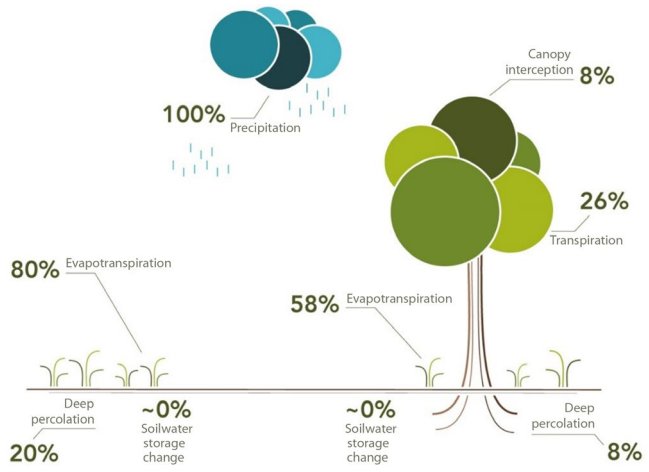

FIGURE 9 Measured rainfall partitioning for grassland and plantation forest in 2013 with unusually high annual rainfall (700 mm). All fluxes are related to annual rainfall

4 | DISCUSSION

4.1 | Environmental control of evaporation

The black locust canopy was well coupled to the atmosphere as the strong relationship between VPD and surface conductance demonstrated (Figure 6). Moreover, the omega factor, which describes the degree of decoupling between transpiration and the saturation deficit in the boundary layer, was on average 0.24 during the main growing seasons (data not shown), indicating that black locust transpiration was strictly physiologically regulated. The results suggest a conservative water use strategy of black locust in avoiding turgor loss and xylem cavitation—supported by the small sensitivity of its canopy conductance and transpiration to rainfall-induced changes in soil moisture conditions (Figure 3). Similar conclusions regarding the water use strategy of black locust stands in Northern China were previously made (Chen et al., 2014; Ma et al., 2017). Chen et al. (2014) investigated transpiration responses to rain pulses in the semiarid part of the Loess Plateau; similar to our study, they found strong control of canopy conductance by VPD on an hourly basis but no firm relationship between daily transpiration and soil moisture. Jiao, Lu, Sun, Ward, and Fu (2016), Zhang, Guan, Shi, Yamanaka, and Du (2015), and Ma et al. (2017) analyzed transpiration of black locust plantations in the Loess Plateau. Their soils contained significantly more sand compared to our study, implying that their potential plant-available soil water was lower. Although their soils were drier than ours, they found no relationship between soil moisture conditions and daily or monthly transpiration. While other transpiration studies in black locust stands of Northern China reported opposite results, they still suggested a strong influence of soil water conditions on transpiration. Jiao, Lu, Fu, et al. (2016) observed that sap flux density of black locust stands increased by 5% and 9% in 12 and 28 year old trees after rainfall, respectively. Du et al. (2011) showed that rainfall-induced increases in soil moisture were accompanied by increases in normalized sap flux densities; for instance, maximum flux density was ~0.57 and ~0.75 on a pre- and post-rainfall day, respectively. However, Du et al. (2011) acknowledged that the differences in VPD and solar radiation (both considerably larger on the post-rainfall day) between the 2 days made it difficult to determine the effect of rainfall on diurnal patterns. These discrepancies might be attributed to differences in available soil water during the measurement periods. As outlined above, the study area experienced above average rainfall. Due to frequent heavy rainfall during both growing seasons, black locust showed no severe water shortage (Figure 1). Thus, no responses of transpiration to rain pulses were detected. However, it is possible that during seasons of below average rainfall soil under black locust dries more intensively and significant responses of transpiration to rainfall-induced increase in plant-available soil water might occur.

Deviating from the general expectation that grass and other short vegetation is decoupled from the atmosphere (Jarvis & Mcnaughton, 1986), our study showed that grassland was moderately coupled to the atmosphere as demonstrated by the analysis of the relationship between evaporation from grassland and net radiation and between surface conductance and VPD (Figures 5 and 7). Moreover, the omega factor was on average 0.47 during the main growing seasons (not shown) indicating moderate coupling between the grass surface and atmosphere. As shown above (Figure 1), Loess Plateau soils are usually quite dry in spring and early summer. Moderate coupling of the grass surface to the atmosphere could thus indicate that grass had partially adapted to the limited soil water availability in spring, with a moderate level of stomatal control of water loss (Figure 7). Our finding is supported by that of De Kauwe, Medlyn, Knauer, and Williams (2017), concerning how different vegetation types control transpiration fluxes based on estimates of the decoupling coefficient derived from FLUXNET data. They found for grasses that the degree of coupling increased significantly with decreasing 3 month rainfall. Compared to grassland, our understory seemed better coupled to the atmosphere as the relationships of evaporation and net radiation with conductance, VPD, and topsoil moisture conditions revealed (Figures 5 and 7). A further indication of the considerable coupling between the understory and atmosphere was the small difference in VPD between forest floor and grassland (Figure 2). However, VPD was not the main driver of understory evaporation—rather, it was radiation—but evaporation rates were controlled by canopy conductance, VPD, and soil moisture. This is discussed in more detail in supplementary material where measured and simulated ET_{us} are compared. The relationship between environmental factors and understory canopy conductance should be considered when modeling evapotranspiration of multilayer forest stands.

Significant understory–atmosphere coupling was also previously found (Black & Kelliher, 1989; Gobin, Korboulewsky, Dumas, & Balandier, 2015; Iida et al., 2009; Jung et al., 2013; Wilson, Hanson, & Baldocchi, 2000). Coupling of the understory to the air above the canopy is due to gusting phenomena. Small eddies or gusts penetrate the canopy from above in short intervals and displace the air equilibrating with the understory (Black & Kelliher, 1989).

4.2 | Reliability of measured water cycle components

The reliability of our sap flow measurements is discussed under data gap filling procedures (supplementary material) and in Schwärzel et al. (2018). Moreover, Ma et al. (2017) and Schwärzel et al. (2018) argued that most previous experimenters significantly underestimated the sap flow of black locust using Granier's universal calibration equation—Equation (3). Investigators (Jian, Zhao, Fang, & Yu, 2015; Ma et al., 2017; Zhang et al., 2018) who modified the Granier method found that black locust transpiration rates were consistent with the generally accepted notion that afforestation resulted in a significant discharge reduction in the Loess Plateau through elevated evapotranspiration (Schwärzel et al., 2018). Ma's and Zhang's studies were comparable to our study in terms of maximum LAI (2.4–2.8) and mean annual rainfall (580–592 mm) whereas mean annual

rainfall was only 420 mm for Jian et al. (2015). The latter quantified stand transpiration of a 28 year old black locust forest (mean LAI ~ 2.5) over a period of 5 years; their average daily transpiration was 1.1 mm, which agrees well with our findings. Ma et al. (2017) reported average daily transpiration values of 2.1 mm for 2015 and 1.6 mm for 2016 for a 15 year old black locust stand, and Zhang et al. (2018) found 1.7 mm for a 10 year old stand. Strikingly, more water evaporated under comparable LAI and climate conditions for younger than older stands. This is because the impact of forests on water resources depends on age, as research on discharge and soil water reduction through afforestation has demonstrated (Liu et al., 2018; Nan, Wang, Jiao, Zhu, & Sun, 2019; Scott & Prinsloo, 2009; Wang et al., 2012).

Understory evaporation was a significant component of the water balance of the studied plantation (Table 2, Figure 8). Similar findings were reported from other forests. Understory vegetation of Mediterranean oak savannas (Dubbert et al., 2014; Paço et al., 2009) and eastern Siberian larch forests can contribute up to 50% of total evaporation (Iida et al., 2009; Kelliher et al., 1997). About 20%–30% of net canopy mass and energy exchange occurred at the floor of boreal pine forest (Baldocchi & Vogel, 1996). Gimeno et al. (2018) reported for mature native eucalyptus woodland in a humid temperate–subtropical transitional climate that the understory contributed 20% of total evapotranspiration. Even in a temperate mixed forest of broadleaved and coniferous species, understory transpiration represented 9% of total evapotranspiration (Soubie, Heinesch, Granier, Aubinet, & Vincke, 2016). To our knowledge, no previous experimenter has quantified overstory and understory fluxes in any black locust stand. Jian et al. (2015) and Jiao et al. (2018) measured soil evaporation under black locust stands planted in the 1980s in the semiarid part of the Loess Plateau—soil water availability was lower than that for our site due to lower rainfall and significantly more sand in the loess. This might be why these two previous studies found that soil under the black locust canopy was partly without understory. Jian et al. (2015) recorded average daily soil evaporation of 1.1 mm during the season and Jiao et al. (2018) observed 0.8 mm. This was lower than our average result of 1.8 mm, but the differences are reasonable considering that our lysimeter simultaneously captured root water uptake and evaporation from soil. Jian et al. (2015) found that soil evaporation accounted for >40% of total seasonal (May–September) forest ETI. Jiao et al. (2018) reported that soil evaporation represented 55%–59% of total seasonal forest ETI. Wang (1992) used water balance to estimate evapotranspiration of a 14 year old black locust stand, and reported annual evapotranspiration of 630 mm for a year with rainfall of 700 mm, consistent with our findings (Table 2).

Comparing seepage estimates using different methods is another means of evaluating the reliability of our measurements. The drainage water collected at the bottom of the lysimeter under forest was 69 mm in 2013 (Table 2), and the corresponding seepage using the ZFP method and calculation as residual of annual water balance were 63 and 56 mm, respectively (Figures 8 and 9). The drainage water from the bottom of the lysimeter under grass was 178 mm in 2013 (Table 2), while the seepage estimate using ZFP was 188 mm (Figure 8) and that calculated using annual water balance was 140 mm (Figure 9). The discrepancy (~20%) between drainage water collected from lysimeters and those calculated using the water balance indicates only small changes in annual soil water storage at our site. The soil pressure head values at a depth of 80 cm were slightly higher at the beginning than at the end of 2013 (Figure 1). However, good agreement between the three seepage estimates indicates that our measurement results are plausible.

Among the few studies that have estimated annual groundwater recharge for the Loess Plateau (Gates, Scanlon, Mu, & Zhang, 2011; Huang & Pang, 2011; Huang, Pang, & Edmunds, 2013; Huang, Pang, Liu, Ma, & Gates, 2017; Huang, Yang, Liu, & Li, 2016; Lin & Wei, 2006), despite the considerable range in mean annual rainfall (360–625 mm) in the case of Huang et al. (2017), for example, recharge to rainfall ratios among sites were similar (6%–18%) and overlaps with seepage ratios estimated for our grassland of 9%–25% (based on Table 2).

4.3 | Dilemma of soil conservation through afforestation

Our field observations at adjacent plantation and grassland sites showed that afforested land removed significantly more water from soil to atmosphere than grassland. Afforestation promotes formation of multilayer stands with higher LAI and deeper root systems, thus increasing evapotranspiration (Table 2; Figure 4). Contrary to common belief, the understory, not the overstory, was the main water consumer in this plantation. The enhanced evapotranspiration of afforested land was at the expense of seepage (Figures 8 and 9; and Table 2). Our measurements indicate that significant seepage under forests might only occur in years with rainfall exceeding the annual average of 590 mm. Moreover, seepage flow below the root zone only occurred during the rainy season of June–September (Figure 8). Our data suggest that preferential flow through the root zone is an important mechanism of seepage formation in the study area. In a study using the chloride mass balance method for recharge estimation under different land covers, Gates et al. (2011) and Huang and Pang (2011) found chloride accumulation under tree and shrub plantations, but not under agricultural land-use, suggesting that afforestation prevents seepage—a conclusion confirmed by our study. This decrease in seepage can be explained by vertical niche separation between trees and grasses. A comparison of soil moisture dynamics between grassland and forest—indicated by the seasonal course of soil pressure head as a function of depth—demonstrated that the understory sourced water from topsoil, while the overstory mainly took water from subsoil (Figure 1). Such a two-source system was proposed by Walter (1939) to explain the equilibrium of trees and grasses in savannas. This concept was later simplified by Walker and Noy-Meir (1982) and described by Ward, Wiegand, and Getzin (2013) as follows—grasses with their intense and shallow root system use water only from subsurface layers while woody savanna

trees use little of the topsoil water but would have exclusive access to and primarily rely on subsoil water below the grass roots, consistent with our study. Due to the vertical niche separation, the soil profile under the forest with understory was much more depleted during the season than under grassland. Thus, more rainwater was needed to recharge plant-available soil water before seepage could occur.

While effective soil erosion control by afforestation can lower surface runoff and "green up" China's drylands, these new forests have resulted in unintended local and regional water shortages, particularly in the Loess Plateau (Wang et al., 2012; Yao, Xiao, Shen, Wang, & Jiao, 2016; Yuan et al., 2018; Zhang, Podlasly, Feger, Wang, & Schwärzel, 2015; Zhang et al., 2014; Zhao, Mu, Strehmel, & Tian, 2014). Rainfall is the primary source of water for plant growth there and the amount of rainfall infiltrating into the soil depends on soil surface conditions; they control the partitioning of rainfall into overland flow and subsurface flow feeding soil water storage (Falkenmark & Rockström, 2006).However, water is not only partitioned at the soil surface but also in the root zone. At the partitioning point in the root zone, water is divided into seepage which eventually contributes to groundwater recharge (blue flow) and into evaporation (green flow; Falkenmark & Rockström, 2006). Compared to grassland, green flow from afforested land is enhanced by the vertical niche separation between overstory and understory. The dilemma of soil erosion control in drylands is clarified in Figure 9. Establishment of vegetation as a measure to reduce soil erosion significantly alters the portion of blue and green flows in water-limited regions. The relative contribution of the different green flow components to total evapotranspiration depends on forest stand structure (e.g., density, LAI, and species composition). Any management-induced changes in this structure (e.g., thinning) thus alter the partitioning of evaporative fluxes and will also lead to a complex change in seepage and water yield (Ganatsios, Tsioras, & Pavlidis, 2010; Jackson et al., 2005; Xuan Dung, Miyata, & Gomi, 2011). To ensure adequate levels of water supply, at both local and regional scales, forest evapotranspiration requires better control by vegetation management (Zhang & Schwärzel, 2017). Our results reveal that ET_{us} of the studied forest needs to be lowered to promote seepage. To increase infiltration and seepage while minimizing water consumption by vegetation for effective forest management, introducing tree species that generate stem flow may increase seepage rates while the understory will be partly overshadowed due to the increase of LAI and so would reduce understory water consumption. Schwärzel, Ebermann, and Schalling (2012) showed that, for beech trees, crown and root architecture control stem-flow formation, stem-flow infiltration, and subsurface transport of stem-flow through soil. As mentioned earlier, 60%–80% of seasonal rainfall in the Loess Plateau is storm events. It is well known that significant stem-flow formation occurs during such events (e.g., Levia & Germer, 2015). Introducing stem-flow-generating tree species (e.g., Chinese walnut) into black locust monocultures may help reduce soil erosion and ET_{us}. Simultaneously, enhanced stem-flow formation could favor increased seepage rates and thus water yield. Such stem-flow-generating tree species could act as a biological rainwater harvesting system for increasing blue water flows. However, to our knowledge, such processes have never been studied in the Loess Plateau.

4.4 | Implications of global reforestation on water cycle

Forest restoration and tree-planting projects must be evaluated against the sustainable use of water resources and related ecological and socioeconomic consequences. From the Great Green Wall initiative in Africa's Sahel region to the Restoration Initiative in Asia, tree-planting is a popular strategy to mitigate climate change (Bastin et al., 2019; Griscom et al., 2017), land desertification and degradation, biodiversity loss, and food deficit. Such programs require large public and private investments, yet their sustainability is often not fully evaluated. The trade-offs between water loss and carbon sequestration have not been acknowledged in many regions (Feng et al., 2016; Jackson et al., 2005). Field research is expensive and hydrologic responses to tree planting takes time to observe. To fully understand how plantation forests alter the water cycle, important hydrological processes, such as seepage and soil and canopy evaporation, need to be fully considered. Where the partition of evapotranspiration is to be understood, its values for both the overstory and understory must be measured at the same time. This study is a pioneering attempt to quantify the impacts of dryland forestland versus grassland on the water cycle and compare their water fluxes addressing this knowledge gap. Our work showed that plantations in an arid/semiarid climate consume an amount of water close to (in normal rainfall years) and likely to exceed (in drier years) the annual precipitation. Planted forests deplete soil water and prevent deep seepage for groundwater recharge, thus, possibly further intensifying local and regional water scarcity and cause conflicts over water supply. This study provides local and national policymakers, NGOs, and UN organizations with evidence that good intentions to implement large-scale tree-planting in drylands can have drawbacks and unintended consequences to local and regional water security. With climate change resulting in more frequent and longer droughts over larger areas, a well-rounded evaluation of the effects of dryland tree-planting on the water cycle and of hydrological feedback is particularly critical and meaningful to avoid high costs (i.e., trade-off of ecosystem services) and loss of valuable investment.

ACKNOWLEDGEMENTS

This study was funded by the Deutsche Forschungsgemeinschaft (DFG Schw1448-3/1). We thank Atiqah Fairuz Salleh for final language editing.

ORCID

Kai Schwärzel https://orcid.org/0000-0002-8295-7919

REFERENCES

Baldocchi, D. D., & Vogel, C. A. (1996). Energy and CO_2 flux densities above and below a temperate broad-leaved forest and a boreal pine forest. *Tree Physiology*, *16*(1–2), 5–16. https://doi.org/10.1093/treephys/16.1-2.5

Bastin, J.-F., Finegold, Y., Garcia, C., Mollicone, D., Rezende, M., Routh, D., … Crowther, T. W. (2019). The global tree restoration potential. *Science*, *365*(6448), 76–79.

Black, T. A., & Kelliher, F. M. (1989). Processes controlling understorey evapotranspiration. *Philosophical Transactions - Royal Society of London, B*, *324*(1223), 207–231.

Bryan, B. A., Gao, L., Ye, Y., Sun, X., Connor, J. D., Crossman, N. D., … Hou, X. (2018). China's response to a national land-system sustainability emergency. *Nature*, *559*(7713), 193–204. https://doi.org/10.1038/s41586-018-0280-2

Chen, C., Park, T., Wang, X., Piao, S., Xu, B., Chaturvedi, R. K., … Myneni, R. B. (2019). China and India lead in greening of the world through land-use management. *Nature Sustainability*, *2*(2), 122–129. https://doi.org/10.1038/s41893-019-0220-7

Chen, J., John, R., Sun, G. E., Fan, P., Henebry, G. M., Fernández-Giménez, M. E., … Qi, J. (2018). Prospects for the sustainability of social-ecological systems (SES) on the Mongolian plateau: Five critical issues. *Environmental Research Letters*, *13*(12), 123004. https://doi.org/10.1088/1748-9326/aaf27b

Chen, L., Zhang, Z., Zeppel, M., Liu, C., Guo, J., Zhu, J., … Zha, T. (2014). Response of transpiration to rain pulses for two tree species in a semiarid plantation. *International Journal of Biometeorology*, *58*(7), 1569–1581. https://doi.org/10.1007/s00484-013-0761-9

Clausnitzer, F., Köstner, B., Schwärzel, K., & Bernhofer, C. (2011). Relationships between canopy transpiration, atmospheric conditions and soil water availability—Analyses of long-term sap-flow measurements in an old Norway spruce forest at the Ore Mountains/Germany. *Agricultural and Forest Meteorology*, *151*(8), 1023–1034. https://doi.org/10.1016/j.agrformet.2011.04.007

Cooper, J., Gardner, C., & Mackenzie, N. (1990). Soil controls on recharge to aquifers. *Journal of Soil Science*, *41*(4), 613–630. https://doi.org/10.1111/j.1365-2389.1990.tb00231.x

De Kauwe, M. G., Medlyn, B. E., Knauer, J., & Williams, C. A. (2017). Ideas and perspectives: How coupled is the vegetation to the boundary layer? *Biogeosciences*, *14*(19), 4435–4453. https://doi.org/10.5194/bg-14-4435-2017

Du, S., Wang, Y.-L., Kume, T., Zhang, J.-G., Otsuki, K., Yamanaka, N., & Liu, G.-B. (2011). Sapflow characteristics and climatic responses in three forest species in the semiarid Loess Plateau region of China. *Agricultural and Forest Meteorology*, *151*(1), 1–10. https://doi.org/10.1016/j.agrformet.2010.08.011

Dubbert, M., Piayda, A., Cuntz, M., Correia, A. C., Costa e Silva, F., Pereira, J. S., & Werner, C. (2014). Stable oxygen isotope and flux partitioning demonstrates understory of an oak savanna contributes up to half of ecosystem carbon and water exchange. *Frontiers in Plant Science*, *5*(OCT). https://doi.org/10.3389/fpls.2014.00530

Falkenmark, M., & Rockström, J. (2006). The new blue and green water paradigm: Breaking new ground for water resources planning and management. *Journal of Water Resources Planning and Management*, *132*(3), 129–132. https://doi.org/10.1061/(ASCE)0733-9496(2006)132:3(129)

Federer, C. A., Vörösmarty, C., & Fekete, B. (2003). Sensitivity of annual evaporation to soil and root properties in two models of contrasting complexity. *Journal of Hydrometeorology*, *4*(6), 1276–1290. https://doi.org/10.1175/1525-7541(2003)004<1276:SOAETS>2.0.CO;2

Feng, X., Fu, B., Piao, S., Wang, S., Ciais, P., Zeng, Z., … Wu, B. (2016). Revegetation in China's Loess Plateau is approaching sustainable water resource limits. *Nature Climate Change*, *6*(11), 1019–1022. https://doi.org/10.1038/nclimate3092

Feng, X. M., Sun, G., Fu, B. J., Su, C. H., Liu, Y., & Lamparski, H. (2012). Regional effects of vegetation restoration on water yield across the Loess Plateau. *China. Hydrology and Earth System Sciences*, *16*(8), 2617–2628. https://doi.org/10.5194/hess-16-2617-2012

Ganatsios, H. P., Tsioras, P. A., & Pavlidis, T. (2010). Water yield changes as a result of silvicultural treatments in an oak ecosystem. *Forest Ecology and Management*, *260*(8), 1367–1374. https://doi.org/10.1016/j.foreco.2010.07.033

Gates, J. B., Scanlon, B. R., Mu, X., & Zhang, L. (2011). Impacts of soil conservation on groundwater recharge in the semi-arid Loess Plateau, China. *Hydrogeology Journal*, *19*(4), 865–875. https://doi.org/10.1007/s10040-011-0716-3

Gimeno, T. E., McVicar, T. R., O'Grady, A. P., Tissue, D. T., & Ellsworth, D. S. (2018). Elevated CO_2 did not affect the hydrological balance of a mature native Eucalyptus woodland. *Global Change Biology*, *24*(7), 3010–3024.

Gobin, R., Korboulewsky, N., Dumas, Y., & Balandier, P. (2015). Transpiration of four common understorey plant species according to drought intensity in temperate forests. *Annals of Forest Science*, *72*(8), 1053–1064. https://doi.org/10.1007/s13595-015-0510-9

Granier, A. (1985). Une nouvelle méthode pour la mesure du flux de sève brute dans le tronc des arbres. *Annales Des Sciences Forestières*, *42*, 193–200. https://doi.org/10.1051/forest:19850204

Griscom, B. W., Adams, J., Ellis, P. W., Houghton, R. A., Lomax, G., Miteva, D. A., … Fargione, J. (2017). Natural climate solutions. *Proceedings of the National Academy of Sciences of the United States of America*, *114*(44), 11645–11650. https://doi.org/10.1073/pnas.1710465114

Huang, T., & Pang, Z. (2011). Estimating groundwater recharge following land-use change using chloride mass balance of soil profiles: A case study at Guyuan and Xifeng in the Loess Plateau of China. *Hydrogeology Journal*, *19*(1), 177–186. https://doi.org/10.1007/s10040-010-0643-8

Huang, T., Pang, Z., & Edmunds, W. M. (2013). Soil profile evolution following land-use change: Implications for groundwater quantity and quality. *Hydrological Processes*, *27*(8), 1238–1252. https://doi.org/10.1002/hyp.9302

Huang, T., Pang, Z., Liu, J., Ma, J., & Gates, J. (2017). Groundwater recharge mechanism in an integrated tableland of the Loess Plateau, northern China: Insights from environmental tracers. *Hydrogeology Journal*, *25*(7), 2049–2065. https://doi.org/10.1007/s10040-017-1599-8

Huang, T., Yang, S., Liu, J., & Li, Z. (2016). How much information can soil solute profiles reveal about groundwater recharge? *Geosciences Journal*, *20*(4), 495–502. https://doi.org/10.1007/s12303-015-0069-3

Huxman, T. E., Wilcox, B. P., Breshears, D. D., Scott, R. L., Snyder, K. A., Small, E. E., … Jackson, R. B. (2005). Ecohydrological implications of woody plant encroachment. *Ecology*, *86*(2), 308–319. https://doi.org/10.1890/03-0583

Iida, S., Ohta, T., Matsumoto, K., Nakai, T., Kuwada, T., Kononov, A. V., … Yabuki, H. (2009). Evapotranspiration from understory vegetation in an eastern Siberian boreal larch forest. *Agricultural and Forest Meteorology*, *149*(6–7), 1129–1139. https://doi.org/10.1016/j.agrformet.2009.02.003

IUSS Working Group WRB. (2006). *World reference base for soil resources 2006 World Soil Resources Reports No. 103*. Rome, Italy: FAO.

Jackson, R. B., Jobbágy, E. G., Avissar, R., Roy, S. B., Barrett, D. J., Cook, C. W., … Murray, B. C. (2005). Trading water for carbon with biological carbon sequestration. *Science*, *310*(5756), 1944–1947. https://doi.org/10.1126/science.1119282

Jarvis, P. G., & Mcnaughton, K. G. (1986). Stomatal control of transpiration: Scaling up from leaf to region. *Advances in Ecological Research*, *15*(C), 1–49. https://doi.org/10.1016/S0065-2504(08)60119-1

Jia, X., Shao, M., Zhu, Y., & Luo, Y. (2017). Soil moisture decline due to afforestation across the Loess Plateau, China. *Journal of Hydrology*, *546*, 113–122. https://doi.org/10.1016/j.jhydrol.2017.01.011

Jian, S., Zhao, C., Fang, S., & Yu, K. (2015). Effects of different vegetation restoration on soil water storage and water balance in the Chinese Loess Plateau. *Agricultural and Forest Meteorology*, *206*, 85–96. https://doi.org/10.1016/j.agrformet.2015.03.009

Jiao, L., Lu, N., Fu, B., Gao, G., Wang, S., Jin, T., … Zhang, D. I. (2016). Comparison of transpiration between different aged black locust (*Robinia pseudoacacia*) trees on the semi-arid Loess Plateau, China. *Journal of Arid Land*, *8*(4), 604–617. https://doi.org/10.1007/s40333-016-0047-2

Jiao, L., Lu, N., Fu, B., Wang, J., Li, Z., Fang, W., … Zhang, L. (2018). Evapotranspiration partitioning and its implications for plant water use strategy: Evidence from a black locust plantation in the semi-arid Loess Plateau, China. *Forest Ecology and Management*, *424*, 428–438. https://doi.org/10.1016/j.foreco.2018.05.011

Jiao, L., Lu, N., Sun, G., Ward, E. J., & Fu, B. (2016). Biophysical controls on canopy transpiration in a black locust (*Robinia pseudoacacia*) plantation on the semi-arid Loess Plateau, China. *Ecohydrology*, *9*(6), 1068–1081. https://doi.org/10.1002/eco.1711

Jung, E.-Y., Otieno, D., Kwon, H., Lee, B., Lim, J.-H., Kim, J., & Tenhunen, J. (2013). Water use by a warm-temperate deciduous forest under the influence of the Asian monsoon: Contributions of the overstory and understory to forest water use. *Journal of Plant Research*, *126*(5), 661–674. https://doi.org/10.1007/s10265-013-0563-5

Kelliher, F. M., Hollinger, D. Y., Schulze, E.-D., Vygodskaya, N. N., Byers, J. N., Hunt, J. E., … Bauer, G. (1997). Evaporation from an eastern Siberian larch forest. *Agricultural and Forest Meteorology*, *85*(3–4), 135–147. https://doi.org/10.1016/S0168-1923(96)02424-0

Khalil, M., Sakai, M., Mizoguchi, M., & Miyazaki, T. (2003). Current and prospective applications of zero flux plane (ZFP) method. *Journal of Japanese Society of Soil Physics*, *95*, 75–90.

Kool, D., Agam, N., Lazarovitch, N., Heitman, J. L., Sauer, T. J., & Ben-Gal, A. (2014). A review of approaches for evapotranspiration partitioning. *Agricultural and Forest Meteorology*, *184*, 56–70. https://doi.org/10.1016/j.agrformet.2013.09.003

Levia, D. F., & Germer, S. (2015). A review of stemflow generation dynamics and stemflow-environment interactions in forests and shrublands. *Reviews of Geophysics*, *53*(3), 673–714. https://doi.org/10.1002/2015RG000479

Lin, R., & Wei, K. (2006). Tritium profiles of pore water in the Chinese loess unsaturated zone: Implications for estimation of groundwater recharge. *Journal of Hydrology*, *328*(1–2), 192–199. https://doi.org/10.1016/j.jhydrol.2005.12.010

Liu, J., Li, S., Ouyang, Z., Tam, C., & Chen, X. (2008). Ecological and socioeconomic effects of China's policies for ecosystem services. *Proceedings of the National Academy of Sciences of the United States of America*, *105*(28), 9477–9482. https://doi.org/10.1073/pnas.0706436105

Liu, Y. U., Miao, H.-T., Huang, Z. E., Cui, Z., He, H., Zheng, J., … Wu, G.-L. (2018). Soil water depletion patterns of artificial forest species and ages on the Loess Plateau (China). *Forest Ecology and Management*, *417*, 137–143. https://doi.org/10.1016/j.foreco.2018.03.005

Lu, P., Urban, L., & Zhao, P. (2004). Granier's thermal dissipation probe (TDP) method for measuring sap flow in trees: Theory and practice. *Acta Botanica Sinica-English Edition*, *46*(6), 631–646.

Ma, C., Luo, Y., Shao, M., Li, X., Sun, L., & Jia, X. (2017). Environmental controls on sap flow in black locust forest in Loess Plateau, China. *Scientific Reports*, *7*(1), https://doi.org/10.1038/s41598-017-13532-8

Nan, G., Wang, N., Jiao, L., Zhu, Y., & Sun, H. (2019). A new exploration for accurately quantifying the effect of afforestation on soil moisture: A case study of artificial Robinia pseudoacacia in the Loess Plateau (China). *Forest Ecology and Management*, *433*, 459–466. https://doi.org/10.1016/j.foreco.2018.10.029

Newman, B. D., Wilcox, B. P., Archer, S. R., Breshears, D. D., Dahm, C. N., Duffy, C. J., … Vivoni, E. R. (2006). Ecohydrology of water-limited environments: A scientific vision. *Water Resources Research*, *42*(6). https://doi.org/10.1029/2005WR004141

Paço, T. A., David, T. S., Henriques, M. O., Pereira, J. S., Valente, F., Banza, J., … David, J. S. (2009). Evapotranspiration from a Mediterranean evergreen oak savannah: The role of trees and pasture. *Journal of Hydrology*, *369*(1–2), 98–106. https://doi.org/10.1016/j.jhydrol.2009.02.011

Podlasly, C., & Schwärzel, K. (2013). Development of a continuous closed pipe system for controlling soil temperature at the lower boundary of weighing field lysimeters. *Soil Science Society of America Journal*, *77*(6), 2157–2163. https://doi.org/10.2136/sssaj2013.03.0113n

Qu, W., Bogena, H. R., Huisman, J. A., & Vereecken, H. (2013). Calibration of a novel low-cost soil water content sensor based on a ring oscillator. *Vadose Zone Journal*, *12*(2), https://doi.org/10.2136/vzj2012.0139

Redei, K., Nicolescu, V.-N., Vor, T., Potzelsberger, E., Bastien, J.-C., Brus, R., … Hernea, C. (2018). Black Locust (*Robinia pseudoacacia* L.), a non-native tree species integrated in European forests and landscapes. An overview. *European Journal of Forest Research*. Retrieved from https://www.bib.irb.hr/967990

Schwärzel, K., Ebermann, S., & Schalling, N. (2012). Evidence of double-funneling effect of beech trees by visualization of flow pathways using dye tracer. *Journal of Hydrology*, *470*, 184–192. https://doi.org/10.1016/j.jhydrol.2012.08.048

Schwärzel, K., Menzer, A., Clausnitzer, F., Spank, U., Häntzschel, J., Grünwald, T., … Feger, K.-H. (2009). Soil water content measurements deliver reliable estimates of water fluxes: A comparative study in a beech and a spruce stand in the Tharandt forest (Saxony, Germany). *Agricultural and Forest Meteorology*, *149*(11), 1994–2006. https://doi.org/10.1016/j.agrformet.2009.07.006

Schwärzel, K., Zhang, L., Strecker, A., & Podlasly, C. (2018). Improved water consumption estimates of black locust plantations in China's Loess Plateau. *Forests*, *9*(4), https://doi.org/10.3390/f9040201

Scott, D. F., & Prinsloo, F. W. (2009). Longer-term effects of pine and eucalypt plantations on streamflow. *Water Resources Research*, *45*(7), https://doi.org/10.1029/2007WR006781

Soubie, R., Heinesch, B., Granier, A., Aubinet, M., & Vincke, C. (2016). Evapotranspiration assessment of a mixed temperate forest by four methods: Eddy covariance, soil water budget, analytical and model. *Agricultural and Forest Meteorology*, *228–229*, 191–204. https://doi.org/10.1016/j.agrformet.2016.07.001

Sun, G., Zhou, G., Zhang, Z., Wei, X., McNulty, S. G., & Vose, J. M. (2006). Potential water yield reduction due to forestation across China. *Journal of Hydrology*, *328*(3–4), 548–558. https://doi.org/10.1016/j.jhydrol.2005.12.013

Walker, B. H., & Noy-Meir, I. (1982). Aspects of the stability and resilience of savanna ecosystems. *Ecology of Tropical Savannas*, *556–590*, https://doi.org/10.1007/978-3-642-68786-0_26

Walter, H. (1939). Grasland, Savanne und Busch der arideren Teile Afrikas in ihrer ökologischen Bedingtheit. *Jahrbücher Für Wissenschaftliche Botanik*, *87*, 750–860.

Wang, Y. (1992). The hydrological influence of black locust plantations in the loess area of northwest China. *Hydrological Processes*, *6*(2), 241–251. https://doi.org/10.1002/hyp.3360060211

Wang, Y., Bredemeier, M., Bonell, M., Yu, P. T., Feger, K. H., Xiong, W., & Xu, L. H. (2012). Comparison between a statistical approach and paired catchment study in estimating water yield response to afforestation. *IAHS Publications*, *353*, 3–11.

Ward, D., Wiegand, K., & Getzin, S. (2013). Walter's two-layer hypothesis revisited: Back to the roots!. *Oecologia*, *172*(3), 617–630. https://doi.org/10.1007/s00442-012-2538-y

Wilson, K. B., Hanson, P. J., & Baldocchi, D. D. (2000). Factors controlling evaporation and energy partitioning beneath a deciduous forest over an annual cycle. *Agricultural and Forest Meteorology*, *102*(2–3), 83–103. https://doi.org/10.1016/S0168-1923(00)00124-6

Xuan Dung, B., Miyata, S., & Gomi, T. (2011). Effect of forest thinning on overland flow generation on hillslopes covered by Japanese cypress. *Ecohydrology*, *4*(3), 367–378. https://doi.org/10.1002/eco.135

Yang, L., Wei, W., Chen, L., & Mo, B. (2012). Response of deep soil moisture to land use and afforestation in the semi-arid Loess Plateau, China. *Journal of Hydrology*, *475*, 111–122. https://doi.org/10.1016/j.jhydrol.2012.09.041

Yao, W., Xiao, P., Shen, Z., Wang, J., & Jiao, P. (2016). Analysis of the contribution of multiple factors to the recent decrease in discharge and sediment yield in the Yellow River Basin. *China. Journal of Geographical Sciences*, *26*(9), 1289–1304. https://doi.org/10.1007/s11442-016-1227-7

Yu, M., Zhang, L., Xu, X., Feger, K.-H., Wang, Y., Liu, W., & Schwärzel, K. (2015). Impact of land-use changes on soil hydraulic properties of Calcaric Regosols on the Loess Plateau, NW China. *Journal of Plant Nutrition and Soil Science*, *178*(3), 486–498. https://doi.org/10.1002/jpln.201400090

Yuan, Z., Yan, D., Yang, Z., Xu, J., Huo, J., Zhou, Y., & Zhang, C. (2018). Attribution assessment and projection of natural runoff change in the Yellow River Basin of China. *Mitigation and Adaptation Strategies for Global Change*, *23*(1), 27–49. https://doi.org/10.1007/s11027-016-9727-7

Zhang, J.-G., Guan, J.-H., Shi, W.-Y., Yamanaka, N., & Du, S. (2015). Interannual variation in stand transpiration estimated by sap flow measurement in a semi-arid black locust plantation, Loess Plateau, China. *Ecohydrology*, *8*(1), 137–147. https://doi.org/10.1002/eco.1495

Zhang, L., Podlasly, C., Feger, K.-H., Wang, Y., & Schwärzel, K. (2015). Different land management measures and climate change impacts on the runoff – A simple empirical method derived in a mesoscale catchment on the Loess Plateau. *Journal of Arid Environments*, *120*, 42–50. https://doi.org/10.1016/j.jaridenv.2015.04.005

Zhang, L., Podlasly, C., Ren, Y., Feger, K.-H., Wang, Y., & Schwärzel, K. (2014). Separating the effects of changes in land management and climatic conditions on long-term streamflow trends analyzed for a small catchment in the Loess Plateau region, NW China. *Hydrological Processes*, *28*(3), 1284–1293. https://doi.org/10.1002/hyp.9663

Zhang, L., & Schwärzel, K. (2017). China's land resources dilemma: Problems, outcomes, and options for sustainable land restoration. *Sustainability*, *9*(12), https://doi.org/10.3390/su9122362

Zhang, Q., Jia, X., Shao, M., Zhang, C., Li, X., & Ma, C. (2018). Sap flow of black locust in response to short-term drought in southern Loess Plateau of China. *Scientific Reports*, *8*(1), https://doi.org/10.1038/s41598-018-24669-5

Zhang, Y., Song, C., Band, L. E., Sun, G., & Li, J. (2017). Reanalysis of global terrestrial vegetation trends from MODIS products: Browning or greening? *Remote Sensing of Environment*, *191*, 145–155. https://doi.org/10.1016/j.rse.2016.12.018

Zhao, G., Mu, X., Strehmel, A., & Tian, P. (2014). Temporal variation of streamflow, sediment load and their relationship in the Yellow River Basin, China. *PLoS ONE*, *9*(3), e91048. https://doi.org/10.1371/journal.pone.0091048

Zhao, G., Mu, X., Wen, Z., Wang, F., & Gao, P. (2013). Soil erosion, conservation, and eco-environment changes in the loess plateau of china. *Land Degradation and Development*, *24*(5), 499–510. https://doi.org/10.1002/ldr.2246

SUPPORTING INFORMATION

Additional supporting information may be found online in the Supporting Information section.

How to cite this article: Schwärzel K, Zhang L, Montanarella L, Wang Y, Sun G. How afforestation affects the water cycle in drylands: A process-based comparative analysis. *Glob Change Biol*. 2020;26:944–959. https://doi.org/10.1111/gcb.14875